



Cite this: DOI: 10.1039/d6ob00369a

Received 4th March 2026,  
Accepted 17th March 2026

DOI: 10.1039/d6ob00369a

rsc.li/obc

## Visible-light-induced regioselective *N*-oxazolidinone radical addition to indoles and arenes *via* EDA complex formation

 Monica Fiorenza Boselli,  †<sup>a</sup> Sara Ferrario,  †<sup>a</sup> Niccolò Intini,  ‡<sup>a</sup>  
 Kirsten Zeitler  <sup>D</sup> and Alessandra Puglisi  \*<sup>a</sup>

We report the generation of *N*-oxazolidinone radicals *via* electron donor–acceptor (EDA) complex formation. Visible light irradiation of pyridinium-based radical precursors, either in the presence or in the absence of NaHCO<sub>3</sub>, enables a mild, regioselective and operationally simple *N*-arylation, providing direct access to *N*-aryloxazolidin-2-ones. The transformation can be easily converted into a continuous flow process, providing improved productivity over the corresponding batch reaction.

Oxazolidin-2-ones are important heterocyclic moieties, commonly found in several pharmaceutical compounds, and they represent the only new class of synthetic antibiotics introduced into clinical use over the past 50 years.<sup>1</sup> Linezolid and Eperezolid are two examples of *N*-arylated oxazolidinones whose antibacterial activity depends on the *N*-aryl substituent. Tremendous advancements in the synthesis of oxazolidin-2-ones have been reported,<sup>2</sup> however, the direct introduction is still challenging. In the past few years, we have developed mild and reliable methodologies to generate *N*-centered radicals under photocatalytic conditions, enabling for the direct formation of C–N bonds.<sup>3–5</sup> In this context, we recently reported the photoredox-catalysed generation of unprecedented *N*-oxazolidinone radicals and their addition to variously functionalized arenes and hetarenes, starting from a novel class of *N*-radical precursors.<sup>6</sup>

Additionally, light-driven synthetic strategies based on the direct irradiative activation of Electron Donor–Acceptor (EDA) complexes have become widely explored in modern organic chemistry.<sup>7–9</sup> Light excitation of the EDA complex may trigger a single-electron-transfer (SET) that can generate radical intermediates under mild, photocatalyst-free conditions.<sup>10</sup> The use of inorganic bases as external electron donors is well docu-

mented in supramolecular chemistry<sup>11</sup> and biological systems.<sup>12</sup> However, their involvement in photochemical transformations has only recently begun to be explored. Exemplarily, in 2017 Leonori and co-workers developed the visible-light-mediated 5-*exo-dig* cyclization reactions of amidyl radicals in the presence of K<sub>2</sub>CO<sub>3</sub> and 1,4-cyclohexadiene.<sup>13</sup> Two years later, Pericàs and co-workers reported a light-driven amidation reaction of (hetero)aromatic systems *via* anion– $\pi$  complex formation between *N*-aryloxyamides, acting as nitrogen radical precursors, and K<sub>2</sub>CO<sub>3</sub>.<sup>14</sup> More recently, Glorius demonstrated the formation of an EDA complex between NaHCO<sub>3</sub> and an *N*-aminopyridinium tetrafluoroborate salt as a nitrogen radical surrogate.<sup>15</sup> Building on these precedents, we report here the EDA complex-mediated *N*-arylation of oxazolidin-2-ones.

The model reaction between *N*-radical precursor **1a**<sup>4,6,16</sup> and 1-methylindole (**2a**) to regioselectively afford compound **3a** was investigated upon blue light irradiation over 16 h under a variety of conditions, including different additives, solvents, stoichiometry and reaction set-ups. Selected results are summarised in Table 1 (for the complete survey of reaction conditions, evaluating additives, reaction time, concentration, solvent system, precursors, stoichiometry see SI).

The results were obtained by evaluating two different batch photoreactors (PRs) (see SI) to increase the efficiency of the transformation: in PR-1 the reaction vials were laterally irradiated by 455 nm blue LEDs, whereas in PR-2 irradiation was provided by a 456 nm Kessil lamp. NaHCO<sub>3</sub> emerged as the most efficient additive when CH<sub>3</sub>CN was used as the solvent. Initial tests showed similar performance of both PRs (Table 1, entries 2 and 4). Although a large excess of NaHCO<sub>3</sub> was initially employed during reaction optimisation (Table 1, entries 1–5), it was found out that 1 equiv. was enough to efficiently promote the radical transformation (Table 1, entry 6). A solvent system water:CH<sub>3</sub>CN (v/v 4:1) was also tested, affording a homogeneous reaction and a good product yield (Table 1, entry 5). Notably, this result may allow to expand the compatibility of the methodology toward water-soluble substrates. An excess of 1-methylindole (**2a**) (2 equiv.), in

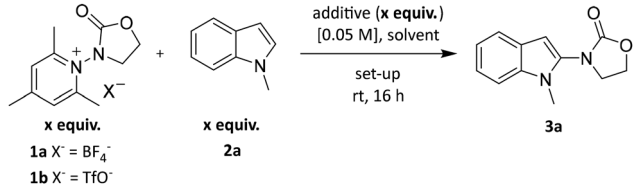
<sup>a</sup>Dipartimento di Chimica, Università degli Studi di Milano, via Golgi, 19-20133 Milano, Italy. E-mail: alessandra.puglisi@unimi.it

<sup>b</sup>Institut für Organische Chemie, Universität Leipzig, Germany

† These authors contributed equally to this work.

‡ Current address: Facultad de Química, Centro de Investigación Multidisciplinar Pleiades-Vitalis, Universidad de Murcia, Spain.



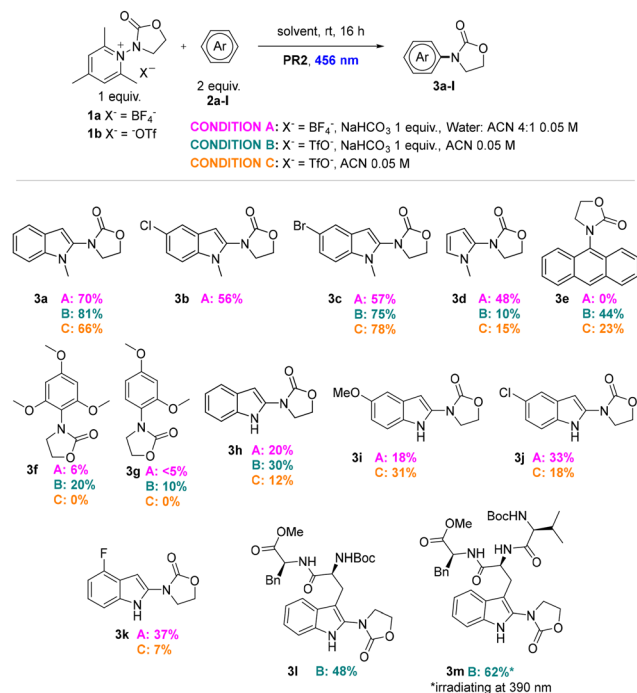
**Table 1** Screening of reaction conditions for the regioselective reaction of **1a** and **2a** in the presence of additives


Entry	Solvent	Additive (equiv.)	Set-up	Ratio <b>1a</b> : <b>2a</b>	Yield <sup>a</sup> (%)
1	CH <sub>3</sub> CN	Na <sub>2</sub> CO <sub>3</sub> (5)	PR-1	1.2 : 1	22
2	CH <sub>3</sub> CN	NaHCO <sub>3</sub> (5)	PR-1	1.2 : 1	60
3	CH <sub>3</sub> CN	KHCO <sub>3</sub> (5)	PR-1	1.2 : 1	8
4	CH <sub>3</sub> CN	NaHCO <sub>3</sub> (5)	PR-2	1.2 : 1	61
5	Water : CH <sub>3</sub> CN 4 : 1	NaHCO <sub>3</sub> (5)	PR-2	1.2 : 1	63
6	Water : CH <sub>3</sub> CN 4 : 1	NaHCO <sub>3</sub> (1)	PR-2	1 : 2	70
7	CH <sub>3</sub> CN	NaHCO <sub>3</sub> (1)	PR-2	1 : 2	78
8 <sup>b</sup>	CH <sub>3</sub> CN	NaHCO <sub>3</sub> (1)	PR-2	1 : 2	81
9 <sup>b</sup>	CH <sub>3</sub> CN	—	PR-2	1 : 2	66
10	CH <sub>3</sub> CN	—	PR-2	1 : 2	Traces

<sup>a</sup> Isolated yield. <sup>b</sup> **1b** was used as radical precursor.

combination with 1 equiv. of NaHCO<sub>3</sub> upon blue irradiation with PR-2 enabled the formation of product **3a** in high yield both under aqueous conditions water : CH<sub>3</sub>CN (v/v 4 : 1) (70%, entry 6) as well as in CH<sub>3</sub>CN (78%, entry 7). It is worth noting that radical precursor **1b**, bearing a triflate (*vs.* BF<sub>4</sub><sup>-</sup>) as the pyridinium counterion, was also highly effective, delivering product **3a** in 81% yield (entry 8).

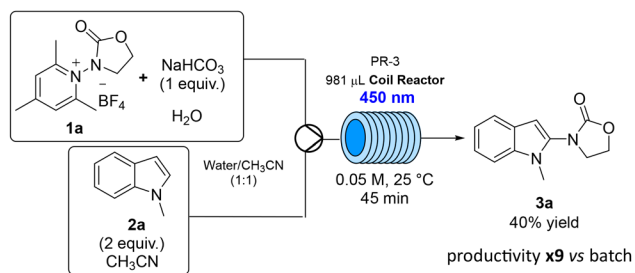
Control experiments revealed that the reaction does not proceed in the absence of light. Working with precursor **1b** under irradiation also allowed formation of product **3a** in 66% isolated yield *in the absence* of NaHCO<sub>3</sub> (Table 1, entry 9), whereas the use of precursor **1a** under identical conditions, only afforded trace amounts of **3a** (entry 10). This interesting finding prompted us to further study the “additive-free” use of precursor **1b** in CH<sub>3</sub>CN under irradiation as *N*-radical source. Having established different conditions to generate the *N*-oxazolidinone radical from precursors **1a** and **1b** (see SI for details), we next explored the scope of the reaction. The results are summarised in Scheme 1. Three different reaction conditions (A–C) were examined under visible-light irradiation (Kessil lamp, 456 nm) for 16 h: precursor **1a**, 1 equiv. of NaHCO<sub>3</sub>, water : CH<sub>3</sub>CN (v/v 4 : 1) 0.05 M (condition A); precursor **1b**, 1 equiv. of NaHCO<sub>3</sub>, CH<sub>3</sub>CN 0.05 M (condition B); precursor **1b**, CH<sub>3</sub>CN 0.05 M (condition C). Differently substituted 1-methylindoles reacted under all three reaction conditions, leading to the corresponding products **3a–c** in satisfactory to high yields. Other electron-rich substrates, including 1-methylpyrrole, anthracene, 1,3,5-trimethoxybenzene and 1,3-dimethoxybenzene, also underwent functionalisation to afford products **3d–g** in moderate to good yields.<sup>17</sup> Moreover, arenes **2e–g** are not prone to form EDA complexes with precursor **1b** (see below for mechanistic investigations). Notably, unprotected indoles also proved to be suitable substrates for the

**Scheme 1** Reaction scope for the regioselective reaction of **1a–b** and **2a–m**.

desired transformation: under the tested conditions, product **3h** was isolated in 12–30% yield. Unprotected indoles bearing either electron-donating or electron-withdrawing groups also underwent the reaction both under condition A and C, although in modest yields (18% and 31% for **3i**, 33% and 18% for **3j**, 37% and 7% for **3k**). The synthetic potential of this methodology was further demonstrated through its application to tryptophan derivatives as reaction partners. Dipeptide Boc-Trp-Phe-OMe afforded the desired product **3l** in 48% yield under condition B, while tripeptide Boc-Val-Trp-Phe-OMe performed very well, delivering product **3m** in 62% yield (under condition B, but irradiating at 390 nm, according to literature precedents for the light-induced modification of tryptophan residues in peptides).<sup>18–20</sup> This highlights the pronounced selectivity of the method for the most electron-rich ring in the substrates, demonstrating its potential application in the late-stage functionalisation of complex biomolecules, under very mild conditions, thus offering further applicability to biological systems.

Given the well-established benefits of light-driven transformations in continuous flow,<sup>21,22</sup> we then further explored the regioselective addition of the *N*-oxazolidinone radical, generated from precursor **1a**, to 1-methylindole (**2a**) in the presence of NaHCO<sub>3</sub> as the external donor under flow conditions using Asia Syrris system (PR-3), equipped with the photochemistry module (for further details, see SI). After extensive reaction conditions optimisation in flow, the following set-up was chosen (Scheme 2): an aqueous solution of **1a** and NaHCO<sub>3</sub> (1 equiv.) and a solution of **2a** (2 equiv.) in CH<sub>3</sub>CN were fed



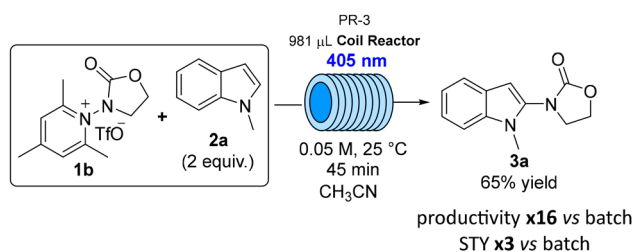


**Scheme 2** Continuous flow reaction using **1a**.

through a T-junction into a coil of 981  $\mu\text{L}$  volume. The final mixture of water and  $\text{CH}_3\text{CN}$  (1 : 1, 0.05 M, homogeneous solution) was irradiated at 450 nm at room temperature. The screening of different residence times (see SI), allowed to identify 45 min as a good compromise between the conversion and the productivity. After a residence time of 45 min, the desired product **3a** was isolated in 40% yield. This led to an increase in productivity of about 9 times compared to the same transformation in batch (57% yield, 16 h).

A more operationally convenient, simple single-feed flow set-up was employed for the reaction using triflate precursor **1b**, with  $\text{CH}_3\text{CN}$  as the solvent (0.05 M). Using the typical 450 nm irradiation, the desired product **3a** was isolated in 50% yield after 45 min residence time. Increasing the residence time up to 60 min was not beneficial, since **3a** was recovered in 51% yield. Gladly, a fine tuning of the reaction conditions allowed to identify 405 nm as optimal wavelength, leading to the isolation of product **3a** in 65% yield in 45 min residence time, as depicted in Scheme 3. Under these flow conditions, the productivity increased of about 16 times compared to the same transformation in batch (50% yield, 16 h) while the space-time yield (STY) was approximately 3 times higher (see SI for details on reaction conditions screening and calculation of productivity and STY).

Investigations were performed in order to provide insights into the reaction mechanism. In particular, UV-Vis absorption spectroscopy<sup>15</sup> was employed to gain insight into the photochemical reaction mechanism either in the presence or in the absence of  $\text{NaHCO}_3$ . UV-Vis spectra of a mixture of pyridinium salt **1a** and 1-methylindole (**2a**) allowed to observe a new absorption band at *ca.* 350 nm (Fig. 1A). The same interaction was observed for precursor **1b** and **2a** (Fig. 1B); a colour



**Scheme 3** Continuous flow reaction using **1b**.

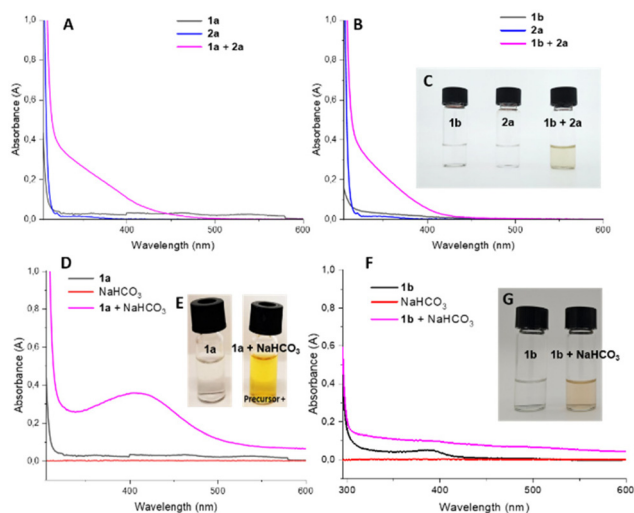


**Fig. 1** (A) UV-Vis absorption spectra of **1a**, **2a** and **1a + 2a**. (B) UV-Vis absorption spectra of **1b**, **2a** and **1b + 2a**. (C) Colourless solution of **1b** (left), **2a** (middle) and yellow solution of **1a** with **2a** (right). (D) UV-Vis absorption spectra of **1a**,  $\text{NaHCO}_3$  and **1a + 1 equiv.** of  $\text{NaHCO}_3$ . (E) Colourless solution of **1a** (left) and yellow solution of **1a** with 1 equiv. of  $\text{NaHCO}_3$  (right). (F) UV-Vis absorption spectra of **1b**,  $\text{NaHCO}_3$  and **1b + 1 equiv.** of  $\text{NaHCO}_3$ . (G) Colourless solution of **1b** (left) and pale-yellow solution of **1b** with 1 equiv. of  $\text{NaHCO}_3$  (right).

change was also observed in the solution of **1b** and **2a** (Fig. 1C). Moreover, UV-Vis spectra showed an evident bathochromic shift for the mixture of nitrogen radical precursor **1a** and  $\text{NaHCO}_3$  compared to the spectrum recorded for **1a** alone, thus hinting to a possible EDA complex formation between the electron-poor precursor **1a** and  $\text{NaHCO}_3$  (Fig. 1D).<sup>13–15</sup> This observation was also in agreement with the observed colour change in the solution of **1a** upon addition of  $\text{NaHCO}_3$  (Fig. 1E). In contrast, mixing the nitrogen radical precursor **1b** with  $\text{NaHCO}_3$  produced a noticeable, albeit less pronounced, change in the UV-Vis spectrum compared to **1b** alone (Fig. 1F). This observation aligns with the less pronounced colour change observed when  $\text{NaHCO}_3$  was added to the solution of **1b** (Fig. 1G). DFT calculations supported the proposal of an electron transfer from the bicarbonate ion to the pyridinium ion (see below and SI for details). Cyclic voltammetry measurements were carried out to compare the electrochemical properties of the two pyridinium salts **1a** and **1b**. Importantly, the different reactivity of precursors **1a** and **1b** can be ascribed to a difference in reaction kinetics, as highlighted by a detailed CV analysis (see SI for detailed studies).

Based on these findings, we propose a plausible mechanism illustrated in Fig. 2 for the transformation. Specifically, the EDA complex formed through the interaction between the electron-poor precursor **1b** and 1-methylindole (**2a**) can be photoexcited under visible-light irradiation. The resulting excited state undergoes a single-electron transfer (SET), leading to the fragmentation of the complex and the subsequent cleavage of radical intermediate **I** to provide 2,4,6-col-



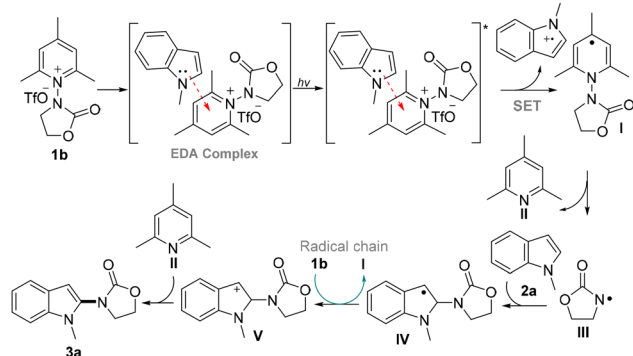


Fig. 2 Proposed reaction mechanism using **1b** as radical precursor.

lidine **II** and the *N*-oxazolidinone radical **III**. The regioselective radical addition of **III** to 1-methylindole (**2a**) affords radical intermediate **IV**, which can engage in a chain propagation step<sup>23,24</sup> by reducing precursor **1b**. Finally, deprotonative rearomatization of the oxidized intermediate **V** affords the desired functionalized indole **3a**.

In the case of radical precursor **1a**, the EDA complex with **2a** is somehow not productive (Table 1, entry 10). In this case, the addition of  $\text{NaHCO}_3$  is beneficial to the reaction initiation, since  $\text{NaHCO}_3$  could act as an external donor for radical precursor **1a**. The EDA complex can then be photoexcited under visible-light irradiation, and the resulting excited state undergoes a single-electron transfer (SET), leading to the fragmentation of the complex and the subsequent cleavage of radical intermediate **I** to provide 2,4,6-collidine **II** and the *N*-oxazolidinone radical **III**. The regioselective radical addition of **III** to 1-methylindole (**2a**) affords radical intermediate **IV**, which – similarly to the mechanism in Fig. 3 – can engage in a chain propagation step by reducing precursor **1a**.<sup>23,24</sup> Finally, rearomatization *via* deprotonation of the oxidized intermediate **V** affords the desired functionalized indole **3a** (Fig. 3). In principle, the mechanism in Fig. 3 could be also plausible for precursor **1b**.

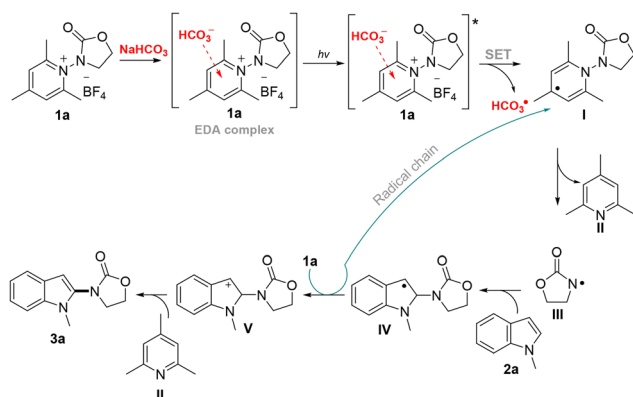


Fig. 3 Proposed reaction mechanism using **1a** as radical precursor.

## Conclusions

In conclusion, a mild and efficient method for the direct *N*-arylation introduction of 2-oxazolidinone on different indoles and arenes *via* EDA complex formation was developed. The reaction efficiently works under a wide variety of conditions and, importantly, allows the employment of unprotected indole moieties offering the opportunity for the direct functionalisation of tryptophan dipeptides and tripeptides. Additionally, the methodology is water compatible, hence importantly expanding the applicability towards water-soluble substrates such as biomolecules. The photochemical reaction can be easily transferred to continuous flow conditions, thus greatly improving the reaction productivity. Mechanistic insights revealed a novel photochemical activation for the pyridinium-derived radical precursors in a photocatalyst-free, simplified set-up. We believe that this work will further advance *N*-oxazolidinone radical chemistry, providing a versatile tool for synthetic chemists aiming to achieve *N*-functionalised oxazolidinones under mild and metal-free conditions.

## Author contributions

Conceptualisation, A. P. and K. Z.; investigation, M. F. B., S. F. and N. I.; writing—original draft preparation, A. P., M. F. B. and S. F.; writing—review and editing, A. P. and K. Z.; supervision, A. P.

## Conflicts of interest

There are no conflicts to declare.

## Data availability

The data supporting this article have been included as part of the supplementary information (SI). Supplementary information: description of equipment, synthesis of substrates **2k** and **2l**, screening of reaction conditions, mechanistic investigation. See DOI: <https://doi.org/10.1039/d6ob00369a>.

## Acknowledgements

This work was supported by: (a) MUSA – Multilayered Urban Sustainability Action – project, funded by the European Union – NextGenerationEU, under the National Recovery and Resilience Plan (NRRP) Mission 4 Component 2 Investment Line 1.5: strengthening of research structures and creation of R&D “innovation ecosystems”, set up of “territorial leaders in R&D”; (b) PSR 2025 grant “Catalytic approaches to the sustainable synthesis of high added-value fine chemicals” from the University of Milan. (c) Deutsche Forschungsgemeinschaft [DFG (German Science Foundation) grant TRR 325-444632635]. The authors thank Alessia Bianchi (Università degli Studi di



Milano) for experimental activity. M. F. B. thanks the Ministero dell'Università e della Ricerca (MUR) (Project PRIN2022 "TECHNO", financed by EU – Next Generation EU, Mission 4 Component 1 CUP G53D23003280006) for a postdoctoral fellowship. S. F. thanks Cosma SpA for cofinancing a PhD fellowship. N. I. thanks Olon SpA for cofinancing a PhD fellowship.

## References

- G. F. S. Fernandes, C. B. Scarim, S. H. Kim, J. Wu and D. Castagnolo, *RSC Med. Chem.*, 2023, **14**, 823–847.
- F. Sun, E. V. Van der Eycken and H. Feng, *Adv. Synth. Catal.*, 2021, **363**, 5168–5195.
- M. F. Boselli, N. Intini, A. Puglisi, L. Raimondi, S. Rossi and M. Benaglia, *Eur. J. Org. Chem.*, 2023, e202201309.
- M. F. Boselli, I. Ghosh, N. Intini, M. Fattalini, A. Puglisi, B. König and M. Benaglia, *Chemistry*, 2025, **31**, e202404385.
- E. Colombo, M. F. Boselli, M. Fattalini, V. Chirolì, S. Rossi, M. Benaglia and A. Puglisi, *Org. Lett.*, 2025, **27**, 8540–8544.
- S. Ferrario, S. Rossi, N. Intini, J. Bruno-Colmenarez, M. Baumann and M. Benaglia, *Org. Lett.*, 2025, **27**, 12276–12280.
- E. F. Hilinski, J. M. Masnovi, C. Amatore, J. K. Kochi and P. M. Rentzepis, *J. Am. Chem. Soc.*, 2002, **105**, 6167–6168.
- C. G. S. Lima, T. d. M. Lima, M. Duarte, I. D. Jurberg and M. W. Paixão, *ACS Catal.*, 2016, **6**, 1389–1407.
- G. E. M. Crisenza, D. Mazzarella and P. Melchiorre, *J. Am. Chem. Soc.*, 2020, **142**, 5461–5476.
- S. V. Rosokha and J. K. Kochi, *Acc. Chem. Res.*, 2008, **41**, 641–653.
- C. Garau, D. Quinonero, A. Frontera, P. Ballester, A. Costa and P. M. Deya, *J. Phys. Chem. A*, 2005, **109**, 9341–9345.
- C. Estarellas, A. Frontera, D. Quinonero and P. M. Deya, *Angew. Chem., Int. Ed.*, 2011, **50**, 415–418.
- D. F. Reina, E. M. Dauncey, S. P. Morcillo, T. D. Svejstrup, M. V. Popescu, J. J. Douglas, N. S. Sheikh and D. Leonori, *Eur. J. Org. Chem.*, 2017, 2108–2111.
- L. Buglioni, M. M. Mastandrea, A. Frontera and M. A. Pericàs, *Chem. Eur. J.*, 2019, **25**, 11785–11790.
- C. C. Chintawar, R. Laskar, D. Rana, F. Schäfer, N. Van Wyngaerden, S. Dutta, C. G. Daniliuc and F. Glorius, *Nat. Catal.*, 2024, **7**, 1232–1242.
- T. W. Greulich, C. G. Daniliuc and A. Studer, *Org. Lett.*, 2015, **17**, 254–257.
- The modest yields of these compounds could be ascribed to the low solubility of the corresponding starting materials under condition A.
- S. J. Tower, W. J. Hetcher, T. E. Myers, N. J. Kuehl and M. T. Taylor, *J. Am. Chem. Soc.*, 2020, **142**, 9112–9118.
- C. R. Hoopes, F. J. Garcia, A. M. Sarkar, N. J. Kuehl, D. T. Barkan, N. L. Collins, G. E. Meister, T. R. Bramhall, C. H. Hsu, M. D. Jones, M. Schirle and M. T. Taylor, *J. Am. Chem. Soc.*, 2022, **144**, 6227–6236.
- M. Hornink, M. E. C. Thedy, E. Romero and G. A. Molander, *ChemistryEurope*, 2026, **4**, e202500284.
- D. Cambie, C. Bottecchia, N. J. Straathof, V. Hessel and T. Noel, *Chem. Rev.*, 2016, **116**, 10276–10341.
- C. Sambigiato and T. Noël, *Trends Chem.*, 2020, **2**, 92–106.
- M. A. Cismesia and T. P. Yoon, *Chem. Sci.*, 2015, **6**, 5426–5434.
- K. A. V. Miyuranga, K. E. Ashcraft and S. P. Pitre, *Tetrahedron Chem*, 2024, **12**, 100110.

